Designation: C1499 – 15

Standard Test Method for Monotonic Equibiaxial Flexural Strength of Advanced Ceramics at Ambient Temperature[1]

This standard is issued under the fixed designation C1499; the number immediately following the designation indicates the year of original adoption or, in the case of revision, the year of last revision. A number in parentheses indicates the year of last reapproval. A superscript epsilon (ε) indicates an editorial change since the last revision or reapproval.

1. Scope

1.1 This test method covers the determination of the equibiaxial strength of advanced ceramics at ambient temperature via concentric ring configurations under monotonic uniaxial loading. In addition, test specimen fabrication methods, testing modes, testing rates, allowable deflection, and data collection and reporting procedures are addressed. Two types of test specimens are considered: machined test specimens and as-fired test specimens exhibiting a limited degree of warpage. Strength as used in this test method refers to the maximum strength obtained under monotonic application of load. Monotonic loading refers to a test conducted at a constant rate in a continuous fashion, with no reversals from test initiation to final fracture.

1.2 This test method is intended primarily for use with advanced ceramics that macroscopically exhibit isotropic, homogeneous, continuous behavior. While this test method is intended for use on monolithic advanced ceramics, certain whisker- or particle-reinforced composite ceramics as well as certain discontinuous fiber-reinforced composite ceramics may also meet these macroscopic behavior assumptions. Generally, continuous fiber ceramic composites do not macroscopically exhibit isotropic, homogeneous, continuous behavior, and the application of this test method to these materials is not recommended.

1.3 The values stated in SI units are to be regarded as standard. No other units of measurement are included in this standard.

1.4 *This standard does not purport to address all of the safety concerns, if any, associated with its use. It is the responsibility of the user of this standard to establish appropriate safety and health practices and determine the applicability of regulatory limitations prior to use.*

2. Referenced Documents

2.1 *ASTM Standards:*[2]

C1145 Terminology of Advanced Ceramics

C1239 Practice for Reporting Uniaxial Strength Data and Estimating Weibull Distribution Parameters for Advanced Ceramics

C1259 Test Method for Dynamic Young's Modulus, Shear Modulus, and Poisson's Ratio for Advanced Ceramics by Impulse Excitation of Vibration

C1322 Practice for Fractography and Characterization of Fracture Origins in Advanced Ceramics

E4 Practices for Force Verification of Testing Machines

E6 Terminology Relating to Methods of Mechanical Testing

E83 Practice for Verification and Classification of Extensometer Systems

E337 Test Method for Measuring Humidity with a Psychrometer (the Measurement of Wet- and Dry-Bulb Temperatures)

F394 Test Method for Biaxial Flexure Strength (Modulus of Rupture) of Ceramic Substrates (Discontinued 2001) (Withdrawn 2001)[3]

IEEE/ASTM SI 10 Standard for Use of the International System of Units (SI): The Modern Metric System

3. Terminology

3.1 *Definitions:*

3.1.1 The definitions of terms relating to biaxial testing appearing in Terminology E6 and Terminology C1145 may apply to the terms used in this test method. Pertinent definitions are listed below with the appropriate source given in parentheses. Additional terms used in conjunction with this test method are defined in the following section.

3.1.2 *advanced ceramic, n*—highly engineered, high performance predominately non- metallic, inorganic, ceramic material having specific functional attributes. **C1145**

[1] This test method is under the jurisdiction of ASTM Committee C28 on Advanced Ceramics and is the direct responsibility of Subcommittee C28.01 on Mechanical Properties and Performance.

Current edition approved July 1, 2015. Published October 2013. Originally approved in 2001. Last previous edition approved in 2013 as C1499 – 09 (2013). DOI: 10.1520/C1499-15.

[2] For referenced ASTM standards, visit the ASTM website, www.astm.org, or contact ASTM Customer Service at service@astm.org. For *Annual Book of ASTM Standards* volume information, refer to the standard's Document Summary page on the ASTM website.

[3] The last approved version of this historical standard is referenced on www.astm.org.

3.1.3 *breaking load, [F], n*—load at which fracture occurs. E6

3.1.4 *equibiaxial flexural strength, [F/L$_2$], n*—maximum stress that a material is capable of sustaining when subjected to flexure between two concentric rings. This mode of flexure is a cupping of the circular plate caused by loading at the inner load ring and outer support ring. The equibiaxial flexural strength is calculated from the maximum-load of a biaxial test carried to rupture, the original dimensions of the test specimen, and Poisson's ratio.

3.1.5 *homogeneous, n*—condition of a material in which the relevant properties (composition, structure, density, etc.) are uniform, so that any smaller sample taken from an original body is representative of the whole. Practically, as long as the geometrical dimensions of a sample are large with respect to the size of the individual grains, crystals, components, pores, or microcracks, the sample can be considered homogeneous.

3.1.6 *modulus of elasticity, [F/L$_2$], n*—ratio of stress to corresponding strain below the proportional limit. E6

3.1.7 *Poisson's ratio, n*—negative value of the ratio of transverse strain to the corresponding axial strain resulting from uniformly distributed axial stress below the proportional limit of the material.

4. Significance and Use

4.1 This test method may be used for material development, material comparison, quality assurance, characterization and design code or model verification.

4.2 Engineering applications of ceramics frequently involve biaxial tensile stresses. Generally, the resistance to equibiaxial flexure is the measure of the least flexural strength of a monolithic advanced ceramic. The equibiaxial flexural strength distributions of ceramics are probabilistic and can be described by a weakest link failure theory, **(1, 2)**[4]. Therefore, a sufficient number of test specimens at each testing condition is required for statistical estimation or' the equibiaxial strength.

4.3 Equibiaxial strength tests provide information on the strength and deformation of materials under multiple tensile stresses. Multiaxial stress states are required to effectively evaluate failure theories applicable to component design, and to efficiently sample surfaces that may exhibit anisotropic flaw distributions. Equibiaxial tests also minimize the effects of test specimen edge preparation as compared to uniaxial tests because the generated stresses are lowest at the test specimen edges.

4.4 The test results of equibiaxial test specimens fabricated to standardized dimensions from a particular material and/or selected portions of a component may not totally represent the strength properties in the entire, full-size component or its in-service behavior in different environments.

4.5 For quality control purposes, results derived from standardized equibiaxial test specimens may be considered indicative of the response of the bulk material from which they were taken for any given primary processing conditions and post-processing heat treatments or exposures.

5. Interferences

5.1 Test environment (vacuum, inert gas, ambient air, etc.) including moisture content (for example, relative humidity) may have an influence on the measured equibiaxial strength. Testing to evaluate the maximum strength potential of a material can be conducted in inert environments and/or at sufficiently rapid testing rates so as to minimize any environmental effects. Conversely, testing can be conducted in environments, test modes and test rates representative of service conditions to evaluate material performance under use conditions.

5.2 Fabrication of test specimens can introduce dimensional variations that may have pronounced effects on the measured equibiaxial mechanical properties and behavior (for example, shape and level of the resulting stress-strain curve, equibiaxial strength, failure location, etc.). Surface preparation can also lead to the introduction of residual stresses and final machining steps might or might not negate machining damage introduced during the initial machining. Therefore, as universal or standardized methods of surface preparation do not exist, the test specimen fabrication history should be reported. In addition, the nature of fabrication used for certain advanced ceramic components may require testing of specimens with surfaces in the as-fabricated condition (that is, it may not be possible, desired or required to machine some of the test specimen surfaces directly in contact with the test fixture). For very rough or wavy as-fabricated surfaces, perturbations in the stress state due to non-symmetric cross-sections as well as variations in the cross-sectional dimensions may also interfere with the equibiaxial strength measurement. Finally, close geometric tolerances, particularly in regard to flatness of test specimen surfaces in contact with the test fixture components are critical requirements for successful equibiaxial tests. In some cases it may be appropriate to use other test methods (for example, Test Method F394).

5.3 Contact and frictional stresses in equibiaxial tests can introduce localized failure not representative of the equibiaxial strength under ideal loading conditions. These effects may result in either over or under estimates of the actual strength **(1, 3)**.

5.4 Fractures that consistently initiate near or just outside the load-ring may be due to factors such as friction or contact stresses introduced by the load fixtures, or via misalignment of the test specimen rings. Such fractures will normally constitute invalid tests (see Note 14). Splitting of the test specimen along a diameter that expresses the characteristic size may result from poor test specimen preparation (for example, severe grinding or very poor edge preparation), excessive tangential stresses at the test specimen edges, or a very weak material. Such fractures will constitute invalid tests if failure occurred from the edge.

5.5 Deflections greater than one-quarter of the test specimen thickness can result in nonlinear behavior and stresses not accounted for by simple plate theory.

[4] The boldface numbers in parentheses refer to the list of references at the end of this standard.

5.6 Warpage of the test specimen can result in nonuniform loading and contact stresses that result in incorrect estimates of the test specimen's actual equibiaxial strength. The test specimen shall meet the flatness requirements (see 8.2 and 8.3) or be specifically noted as warped and considered as a censored test.

6. Apparatus

6.1 *Testing Machines*—Machines used for equibiaxial testing shall conform to the requirements of Practices E4. The load cells used in determining equibiaxial strength shall be accurate within ±1 % at any load within the selected load range of the testing machine as defined in Practice E4. Check that the expected breaking load for the desired test specimen geometry and test material is within the capacity of the test machine and load cell. Advanced ceramic equibiaxial test specimens require greater loads to fracture than those usually encountered in uniaxial flexure of test specimens with similar cross sectional dimensions.

6.2 *Loading Fixtures for Concentric Ring Testing*—An assembly drawing of a fixture and a test specimen is shown in Fig. 1, and the geometries of the load and support rings are given in Fig. 2.

6.2.1 *Loading Rods and Platens*—Surfaces of the support platen shall be flat and parallel to 0.05 mm. The face of the load rod in contact with the support platen shall be flat to 0.025 mm. In addition, the two loading rods shall be parallel to 0.05 mm per 25 mm length and concentric to 0.25 mm when installed in the test machine.

6.2.2 *Loading Fixture and Ring Geometry*—Ideally, the bases of the load and support fixtures should have the same outer diameter as the test specimen for ease of alignment. Parallelism and flatness of faces as well as concentricity of the load and support rings shall be as given in Fig. 2. The ratio of the load ring diameter, D_L, to that of the support ring, D_S, shall be $0.2 \le D_L/D_S \le 0.5$. For test materials exhibiting low elastic modulus ($E < 100$ GPa) and high strength ($\sigma_f > 1$ GPa) it is recommended that the ratio of the load ring diameter to that of the support ring be $D_L/D_S = 0.2$. The sizes of the load and support rings depend on the dimensions and the properties of the ceramic material to be tested. The rings are sized to the thickness, diameter, strength, and elastic modulus of the ceramic test specimens (see Section 8). For test specimens made from typical substrates ($h \approx 0.5$ mm), a support ring diameter as small as 12 mm may be required. For test specimens to be used for model verification, it is recommended that the test specimen support diameter be at least 35 mm. The tip radius, r, of the cross sections of the load and support rings should be $h/2 \le r \le 3h/2$.

6.2.3 *Load and Support Ring Materials*—For machined test specimens (see Section 8) the load and support fixtures shall be made of hardened steel of $HR_C > 40$. For as-fabricated test specimens, the load/support rings shall be made of steel or acetyl polymer.

6.2.4 *Compliant Layer and Friction Elimination*—The brittle nature of advanced ceramics and the sensitivity to misalignment, contact stresses and friction may require a compliant interface between the load/support rings and the test specimen, especially if the test specimen is not flat. Line or point contact stresses and frictional stresses can lead to crack initiation and fracture of the test specimen at stresses other than the actual equibiaxial strength.

6.2.4.1 *Machined Test Specimens*—For test specimens machined according to the tolerance in Fig. 3, a compliant layer is not necessary. However, friction needs to be eliminated. Place a sheet of carbon foil (~0.13 mm thick) or Teflon tape (~0.07 mm thick) between the compressive and tensile surfaces of the test specimen and the load and support rings.

NOTE 1—Thicker layers of carbon foil or Teflon tape may be used, particularly for very strong plates. However, excessively thick layers will redistribute the contact region and may affect results. The thicknesses

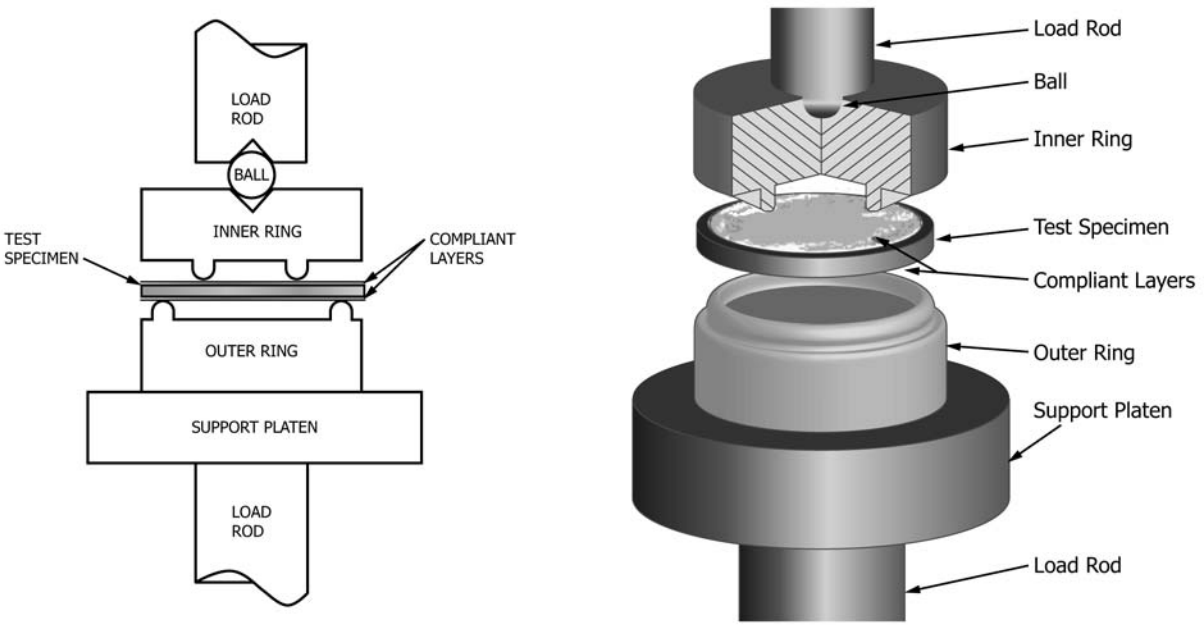

FIG. 1 Section View and Perspective View of Basic Fixturing and Test Specimen for Equibiaxial Testing

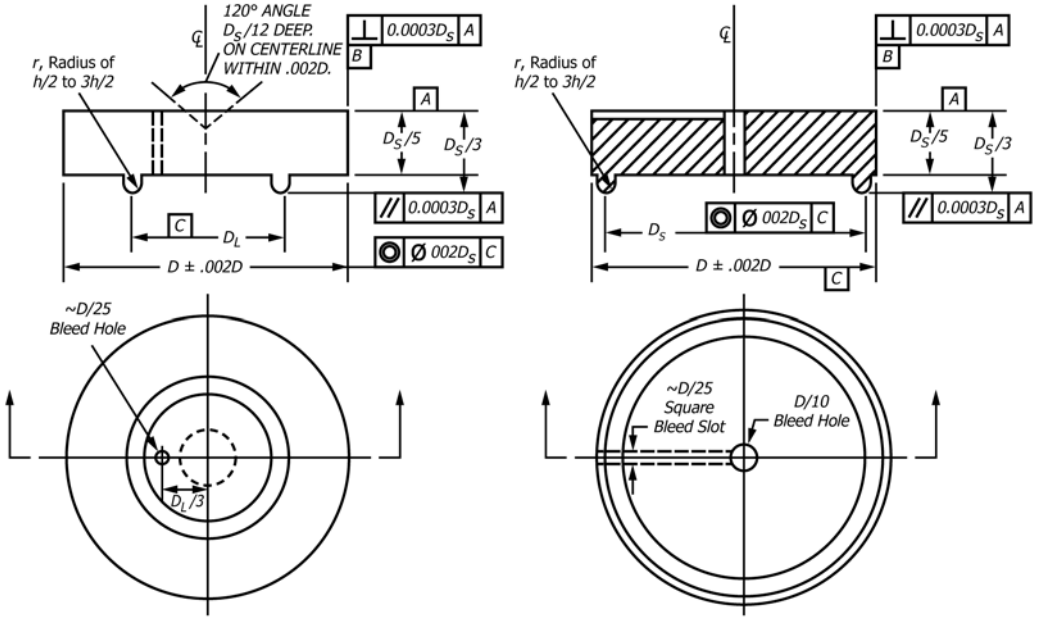

NOTE 1—0.4 to 0.8 μm surface finish. Harden to 40 Rc or greater.

FIG. 2 Load and Support Fixture Designs for Equibiaxial Testing

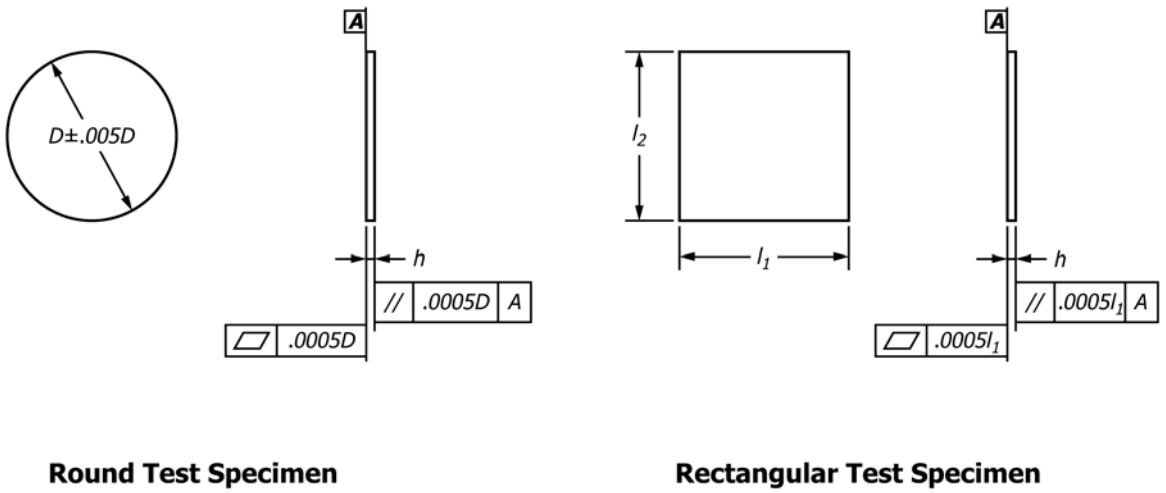

FIG. 3 Recommended Equibiaxial Test Specimen Geometry (*h* and *D* or l_1 and l_2 are Determined from Eq 1-3).

listed above have been used successfully. Guidance regarding the use of thick layers cannot be given currently; some judgement may be required.

Alternatively, an appropriate lubricant (anti-seizing compound or Teflon oil) may be used to minimize friction. The lubricant should be placed only on the load and support rings so that effects of the test environment are not significantly altered. To aid fractographic examination, place a single strip of adhesive tape with a width of D_L or greater on the compressive face of the test specimen. Do not use multiple strips of tape, or a strip of tape with width less than D_L, as this may result in nonuniform loading.

6.2.4.2 *As-Fabricated Test Specimens*—If steel load and support rings are used to test as-fabricated test specimens (for example, as-fired ceramics and glass test specimens), minimize the effects of test specimen-ring misalignment by placing a sheet of rubber or silicone (shore hardness of 60 ± 5) of approximately one-half the test specimen thickness between the test specimen and the support ring. To aid fractographic examination, place a single strip of adhesive tape with a width of D_L or greater on the compressive face of the test specimen. Do not use multiple strips of tape, or a strip of tape with width less than D_L, as this may result in nonuniform loading. To minimize the effects of friction at the load ring interface, place a sheet of carbon foil or TFE-fluorocarbon tape between the compressive surface of the test specimen and the load-ring. Alternatively, an appropriate lubricant (anti-seizing compound or TFE-fluorocarbon oil) may be used to minimize friction at the load ring. If acetyl polymer load rings are used, a compliant layer is not required. Minimize the effects of friction at the load

ring interface, by placing a sheet of carbon foil or TFE-fluorocarbon tape between the compressive and tensile surfaces of the test specimen and the load and support rings. Alternatively, an appropriate lubricant (anti-seizing compound or TFE-fluorocarbon oil) may be used to minimize friction at the load ring.

NOTE 2—As-fabricated test specimens that meet the flatness requirements in Fig. 3 may be tested as described in 6.2.4.1. A compliant layer is not necessary.

NOTE 3—The use of acetyl polymer load rings can result in sufficiently low friction (**4**) so that no layer is required. If the friction coefficient is less than 0.05, then the friction reduction layer may be eliminated.

6.3 *Alignment*—The load ring and support ring shall be aligned concentrically to 0.5 % of the support ring diameter. The test specimen shall be concentric with the load and support rings to 2 % of the support ring diameter.

6.4 *Allowable Deflection*—Excessive deflections can result in a calculated equibiaxial strength different than the actual equibiaxial strength. The test specimens allowed in this standard are designed to avoid excessive deflection (**3, 5-7**). Measurement of deflection is not required, however, center-point deflection can be measured using a deflectometer mounted in the test fixturing (Practice E83). Load-point deflection also may be measured via the test machine actuator, however, appropriate corrections for the test system compliance may need to be applied to the deflection data. Alternatively, deflection can be estimated via the elastic solutions given in section 10.1.

6.5 *Data Acquisition*—At the minimum, obtain an autographic record of applied load versus time. Either analog chart recorders or digital data acquisition systems can be used for this purpose although a digital record is recommended for ease of later data analysis. Ideally, an analog chart recorder or plotter should be used in conjunction with the digital data acquisition system to provide an immediate record of the test as a supplement to the digital record. Recording devices shall be accurate to within ±1 % of the selected range for the testing system including readout unit, as specified in Practice E4, and shall have a minimum data acquisition rate of 10 Hz with a rate of 50 Hz preferred for the rates recommended in 9.2.2. If faster loading rates are used, then use an acquisition rate adequate to provide an error less than ±1 % in the load reading.

6.5.1 Record crosshead displacement of the test machine or time similarly to the load or as independent variables of load.

6.6 *Dimension-Measuring Devices*—Micrometers and other devices used for measuring linear dimensions shall be accurate and precise to at least one half the smallest unit to which the individual dimension is required to be measured. For measuring the thickness, a micrometer with flat anvil faces a resolution better than or equal 0.002 mm is required. Ball-tipped or sharp anvil micrometers are not allowed because localized damage (for example, cracking) can be induced.

NOTE 4—Thickness measurement is especially critical to the calculation of the strength when the test specimens are less than 1 mm thick.

7. Precautionary Statement

7.1 Fractures of loaded advanced ceramics can occur at large loads and high strain energies. To prevent the release of uncontrolled fragments, polycarbonate shielding or equivalent is recommended for operator safety and to capture test specimen fragments to aid fractography.

7.2 Fractures can create fine particles that may be a health hazard. Materials containing whiskers, small fibers or silica particles may also cause health hazards. For such materials, the operator is advised to consult the material safety data sheet for guidance prior to testing. Suitable ventilation or masks may be warranted.

8. Test Specimens

8.1 *Test Specimen Dimensions*—Fig. 3 illustrates test specimen geometry. The relative dimensions are chosen to ensure behavior reasonably described by simple plate theory. Choose the dimension such that the test specimen thickness, h, in units of mm, is

$$\frac{D_S}{10} \geq h \geq \sqrt{2\sigma_f D_S^2/3E} \tag{1}$$

where:

D_S = the support ring diameter in units mm,
σ_f = the expected equibiaxial fracture strength in units MPa, and
E = the modulus of elasticity in units MPa (Test Method C1259).

Choose the test specimen and support ring diameters such that the difference in diameters (D–D_S) is

$$2 \leq \frac{D - D_S}{h} \leq 12 \tag{2}$$

where:

D = the test specimen diameter in units of mm for circular test specimens.

NOTE 5—For test specimens machined according to 8.2.3, a non-dimensionalized overhang of $(D–D_S)/h = 2$ is generally sufficient. However, for test specimens that are scored from larger plates or for test specimens with poor edge finish, a non-dimensionalized overhang of $(D–D_S)/h = 12$ may be required. For optical materials, non-dimensionalized overhang larger than 12 may be required, and it is recommended that at least $(D–DS)/h = 3$ be used. Eq 7 is valid for overhangs as large as $(D–D_S)/h = 24$. However, such large overhang substantially alters the stress distribution, and tests performed with large overhang may result in substantially different measured strengths than tests performed with much smaller overhang. Thus, overhang of $(D–D_S)/h \leq 24$ is allowed. However, it is recommended that $(D–D_S)/h \leq 12$ be used. The edge stress for $D_S/h = 10$ varies from ~30 % to ~50 % of the maximum stress as $(D–D_S)/h$ varies from 12 to 2, respectively. For $D_S/h = 30$, the edge stress varies from~12% to~40% of the maximum stress as $(D–D_S)/h$ varies from 12 to 2, respectively (**8**). The exact solution for the tangential stress at the edge of a circular plate (**9**) can be calculated from:

$$\sigma_e = \frac{3F(1-v)(D^2{}_s - D^2{}_L)}{2\pi h^2 D^2}$$

where the variables are as defined in Eq 1 and Eq 2.

It is recommended that the test specimens be circular, however, in some cases it is advantageous to fabricate rectangular test specimens. For a rectangular test specimen, the value of D for calculations with Eq 1 and Eq 2 is:

$$D = 0.54(l_1 + l_2) \tag{3}$$

where:

l_1 *and* l_2 = the lengths of the edges. The edge lengths should be within $0.98 \leq l_1/l_2 \leq 1.02$.

8.2 *Test Specimen Preparation: Machined Test Specimens*—A variety of surface preparations are acceptable. Unless the process used is proprietary, report specifics about the stages of material removal, wheel grits, wheel bonding, amount of material removed per pass, and type of coolant used. Regardless of the procedure used to machine the tensile surface of the test specimen, the flatness of the faces as well as the flatness of the edges shall be as specified in Fig. 3.

8.2.1 *Application-Matched Machining*—The tensile face of the equibiaxial test specimen will have the same surface/edge preparation as that given to a service component.

NOTE 6—An example of application matched machining is blanchard grinding of electronic substrates. Although damage may exist, it is acceptable as the component has such damage in its application.

8.2.2 *Customary Practices*—In instances where a customary machining procedure has been developed that is completely satisfactory for a class of materials (that is, it induces negligible surface/subsurface damage or residual stresses), this procedure may be used to machine the equibiaxial test specimens.

NOTE 7—Uniaxial surface grinding creates surface and subsurface microcracks, which may (or may not) be the strength-controlling flaws. Such machining cracks usually are oriented relative to the grinding direction and consequently may cause a pronounced variation in the uniaxial strength as a function of the test specimen orientation. If machining flaws dominate, equibiaxial test specimens will fail from the worst orientation and the measured equibiaxial strength will be representative of the machining damage. Further, the equibiaxial strength data may not correlate well with uniaxial data generated with standardized procedures that minimize the effects of such populations (**10**). Lapping or annealing can be used to minimize such effects in both equibiaxial strength tests and advanced ceramic components subjected to multiaxial stresses. Lapping needs to be sufficiently deep to remove machining damage (typically 10 to 30 μm deep). Note that surface finish is not a good indicator of the absence of machining damage.

8.2.3 *Recommended Procedure*—In instances where 8.2.1 or 8.2.2 are not appropriate, 8.2.3.1 – 8.2.3.4 shall apply.

8.2.3.1 Perform all grinding or cutting with ample supply of appropriate filtered coolant to keep the test specimen and grinding wheel constantly flooded and particles flushed. Grinding can be done in two stages, ranging from coarse to fine rates of material removal. All cutting can be done in one stage appropriate for the depth of cut.

8.2.3.2 The stock removal rate shall not exceed 0.03 mm per pass to the last 0.06 mm of material removed. Final finishing shall use diamond tools between 320 and 500 grit. No less than 0.06 mm shall be removed during the final finishing stage, and at a rate less than 0.002 mm per pass. Remove equal stock from opposite faces.

8.2.3.3 Grinding is followed by either annealing or lapping, as deemed appropriate.

NOTE 8—For alpha silicon carbide, annealing at ~1200°C in air for ~2 hours was sufficient to heal the grinding damage induced by the procedure in 8.2.3.2 without otherwise altering the material's strength (**10**). However, note that annealing can significantly alter a material's properties (**11**, **12**), and specific procedures will need to be developed for each material.

NOTE 9—For lapping of alpha silicon carbide, the following procedure was successful in elimination of machining damage induced by uniaxial grinding: successive lapping with 15, 9 and 6 μm diamond pastes for ~30, ~25 and ~15 minutes respectively (**13**). Approximately 10 μm of materials was removed. For tungsten carbide, successive machine lapping with 15 and 6 μm diamond pastes for ~60 and ~30 minutes, respectively, with a pressure of ~13.8 kPa was sufficient (**14**). Specific procedures will need to be developed for other materials.

8.2.3.4 To aid in post failure fractographic examination, it is recommended that the orientation of the grinding direction be marked on the test specimens. This can be accomplished with an indelible marker.

8.3 *Test Specimen Preparation: As-Fabricated Test Specimens*—In order to simulate the surface condition of an application in which no machining is used, limited testing of as-fabricated surfaces is allowed and precautions are recommended. The test specimen should be flat to 0.1 mm in 25 mm. For test specimens exhibiting less flatness, it is suggested that the user consider Test Method F394 or the use of fixturing designed to accommodate warped test specimens (for example, (**15**)). Data generated via this standard from test specimens with flatness tolerance exceeding 0.1 mm in 25 mm should be noted as warped and used only for comparison and quality control purposes.

8.4 *Edge Preparation*—Edge failure can be minimized by using the machining practice described in section 8.2.3. Additional beveling or edge preparation is not necessary. However, for as-fabricated test specimens exhibiting poor edge finish or for test specimens made from materials that are particularly difficult to machine without chipping of the edges, edge related failures can be minimized by using the overhang described in Eq 2 or by beveling the test specimen's tensile edge (that is, the edge of the face in contact with the support ring). If edge failures are a concern, it is recommended that the edge on the tensile face be inspected at ~30× magnification and any observed chips removed by beveling.

NOTE 10—For polycrystalline ceramics such as dense silicon carbides, silicon nitrides and aluminas, beveling can be accomplished by hand with 400-grit silicon carbide abrasive paper. Alternatively, a ~0.125 mm, 45° bevel can be ground onto the tensile edge according to the procedures in section 8.2.3. The grinding direction should be circumferential for circular test specimens and parallel to the edges for square test specimens. For softer materials or extremely strong materials, other methods may need to be developed.

8.5 *Handling Precaution*—Exercise care in storage and handling of test specimens to minimize the introduction of severe, extrinsic flaws. In addition, give attention to pre-test storage of test specimens in controlled environments or desiccators to avoid unquantifiable environmental degradation of test specimens prior to testing.

8.6 *Number of Test Specimens*—A minimum of 10 test specimens tested validly is required for the purpose of estimating a mean biaxial flexural strength. For the estimation of the Weibull parameters, a minimum of 30 test specimens validly tested is recommended. However, Practice C1239 should be consulted to determine if the resultant confidence intervals are adequate for the intended purpose. If material cost or test specimen availability limits the number of tests to be conducted, fewer tests may be conducted.

8.7 *Valid Tests*—A valid individual test is one that meets all the following requirements: (*1*) all the testing requirements of this test method, and (*2*) failure does not occur from the test specimen edges. Those tests failing from flaws at the edges, while not valid, may be interpreted as interrupted tests for the purpose of censored test statistical analyses or as an indicator of edge condition.

9. Procedure

9.1 *Test Specimen and Ring Dimensions*—Measure the load and support ring diameters to within 0.2 % of *D*. Determine the test specimen diameter to 0.2 % of *D* by measuring at two radial positions nominally separated by 90°. For square test specimens, determine the width l_1 and length l_2 to 0.2 % at the middle of the edges. Diameter measurements can be made with a digital caliper, optical device (for example, machinists microscope) or a micrometer. In either case the resolution of the instrument shall be better than or equal to 0.01 mm. Measure the thickness to 0.5 % of *h* at the test specimen center and at four equally spaced positions on a diameter nominally equal to that of the support ring. If the test specimen faces are deemed to be parallel, then fewer thickness measurements may be made. To avoid damage in the critical gage section area, use a flat, anvil-type micrometer to measure the thickness. Exercise extreme caution to prevent damage to the test specimen. Alternatively, if damage is a concern even with an anvil-type micrometer, measure the thickness at the four support diameter positions prior to the test for setup purposes and measure the thickness near the test specimen center after the test. Highly polished optical materials can easily be damaged during contact based measurements. Thus any measurements of such materials should be after testing or by using a non-contacting technique. Record and report the measured dimensions. Use the average of the multiple measurements in the equibiaxial stress calculations.

9.1.1 Conduct inspection and measurements of all the test specimens and test specimen dimensions to assure compliance with the specifications of this test method.

9.1.2 Measurement of surface finish is not required; however, such information is desirable. Methods such as contacting profilometry can be used to determine surface roughness of the test specimen faces. If a contacting method is used, exercise caution to avoid causing surface damage to the test specimen. When quantified, report surface roughness and direction of the measurement with respect to the test specimen reference mark (see 8.2.3.4).

9.2 *Test Modes and Rates:*

9.2.1 *General*—Test modes and rates can have distinct influences on fracture behavior of advanced ceramics even at ambient temperatures. Test modes may involve load or displacement control. The recommended rates of testing are intended to be sufficiently rapid to nominally obtain the maximum equibiaxial strength at fracture of the material in the test environment considered. However, rates other than those recommended here may be used to evaluate rate effects. In all cases report the test mode and rate.

9.2.2 *Displacement Rate*—Displacement mode is defined as the control of, or free-running displacement of, the test machine actuator or crosshead. Different test specimen sizes require different displacement rates for a specified stress rate. Stress rates >30-35 MPa/s are recommended. The required displacement rate can be related to the maximum stress rate in the concentric ring test specimen as follows:

$$\dot{\delta} \cong \left(\frac{D_S^2}{6Eh} \right) \dot{\sigma} \tag{4}$$

where:

$\dot{\delta}$ = the displacement rate of the actuator or cross head in units of mm/s, and

$\dot{\sigma}$ = the maximum value of the nominal recommended (or desired) stress rate occurring within the test specimen in units of MPa/s.

The other variables are as defined for Eq 1.

NOTE 11—The use of Eq 4 assumes that the test system compliance is small relative to that of the test specimen. If a compliant layer is used, the actual stressing rate will be lower and may be determined from the slope of a plot of load versus time. For the specific stress rate desired, the displacement rate can be increased to provide the desired stress rate.

9.2.3 *Load Rate*—For test systems employing closed loop controllers, a load rate can be directly applied to the test specimen. The load rate for a stress rate is calculated as follows:

$$\dot{F} = \left(\frac{2}{3}\pi h^2 \left[(1-\nu) \frac{D_S^2 - D_L^2}{2D^2} + (1+\nu) ln \frac{D_S}{D_L} \right]^{-1} \right) \dot{\sigma} \tag{5}$$

where:

$\dot{F}$ = the required load rate in units of N/s,

D_L = the load ring diameter, and

ν = Poisson's ratio (Test Method C1259).

The other variables are as defined for Eq 1 and Eq 4. Alternatively, stress or load rates can be selected to minimize environmental effects when testing in ambient air by producing final fracture in 10 to 15 s:

$$t_f = \sigma_f / \dot{\sigma} \tag{6}$$

where:

t_f = time to fracture in units of s.

9.3 *Conducting the Equibiaxial Strength Test—*

9.3.1 Apply cellophane tape to the compressive surface of the test specimen to retain fracture fragments. The tape should be sufficiently wide to completely cover the test specimen face. Trim excess tape as necessary to avoid interference or handling problems. Take care not to damage the tensile surface or tensile edge of the test specimen.

NOTE 12—Alternatively, fractography can be aided by drawing lines on the compressive surface of the test specimen with an indelible marker or a pencil.

9.3.2 *Compliant Layer/Friction Reducing Layer*—The diameter of the compliant layer and friction reduction layer should be sufficient to cover the outer diameter of the respective ring, but not be so large as to interfere with test specimen/fixture alignment. It is recommended that a hole of diameter ~D_S/2 be cut in the center of the layer in contact with the support ring to allow exposure to the test environment.

9.3.3 *Aligning the Test Specimen*—The primary concern during testing is that the two load rings be concentric (to 0.5 % of the support ring diameter) and parallel to the test specimen faces. Prior to each test, inspect the load rings. Remove any

nicks in the load and support rings (for example,, polish the surfaces with emery cloth) and clean the surfaces with a suitable solvent (for example, alcohol). Assemble any compliant layer, friction reducing layer, the test specimen and load and support rings. If lubricant is use to eliminate friction, apply it to the rings prior to assembly. Align the test specimen and fixtures. Slowly move the actuator or crosshead until a small preload is developed (for example, ~10 % of the failure load). Remove the alignment system (that is, V-blocks) and report the preload.

9.3.4 *Preparations for Testing*—Set the test mode and test rate on the test machine. Ready the autograph and data acquisition systems. Install the protective shield (see 7.1) for containment of fragments and activate the ventilation systems as required.

NOTE 13—If an extensometer is used to monitor bending, it should be zeroed without a preload applied This will ensure that displacement due to the initial loading is observed.

9.3.5 *Conducting the Test*—Initiate the data acquisition. Initiate the test mode. After test specimen fracture, disable the action of the test machine and the data acquisition system. Report the measured breaking load to an accuracy of ±1 % of the load range. Carefully collect any test specimen fragments from the fixturing. Place the test specimen fragments into a suitable, non-metallic container for later analysis.

9.3.6 Determine the ambient temperature and relative humidity at the end of the test in accordance with Test Method E337.

9.3.7 *Post-Test Interpretation*—For a properly conducted equibiaxial test, fracture should typically occur on the tensile surface within the diameter of the load-ring. Some fractures may also initiate from the region between the load ring and the support load ring. Frequent fracture at or near the load ring/test specimen interface implies excessive contact or friction stresses, or fixture/test specimen misalignment.

NOTE 14—Legitimate fracture may occur from outside the inner loading ring, especially in materials with a low Weibull modulus. In such cases, the disk strength reported is nonetheless based on the maximum stress that the disk sustained. In some instance, for example fracture mirror or fracture toughness calculations, the fracture stress used in the calculations is that at the failure origin.

9.4 *Post-Test Validation*—Fractographic examination of the test specimens is recommended to determine the location of test specimen fracture (Practice C1322). In particular, remnants should be examined for evidence of edge-related fractures or repeated fractures near the load ring. Edge fracture indicates an invalid test (see Fig. 4). If the test specimens were machined by uniaxial grinding, it is recommended that the orientation of test specimens primary fracture plane relative to the grinding lay be determined. Repeated fracture parallel to the grinding lay implies the presence of significant machining damage.

10. Calculation of Results

10.1 *Equibiaxial Strength*—The formula for the equibiaxial strength, σ_f, of a circular plate in units of MPa is (**6**, **7**):

$$\sigma_f = \frac{3F}{2\pi h^2}\left[(1-\nu)\frac{D_S^2 - D_L^2}{2D^2} + (1+\nu)ln\frac{D_S}{D_L}\right] \quad (7)$$

where:

F = the breaking load in units of N. The other symbols are as defined in Eq 1 and Eq 5 in mm.

NOTE 15—The estimated strength of a plate is a weak function of Poisson's ratio, and reasonably accurate values should be used. An error of ~25 % in ν (use of $\nu = 0.21$ for a material with $\nu = 0.17$) results in an error of ~2 % in the estimated stress, and an error of ~1 % in the effective area for $m = 4$, where m is the Weibull modulus. A ~50 % error in ν (use of $\nu = 0.26$ for a material with $\nu = 0.17$) results in an error of ~4 % in the estimated stress, and an error of ~1 % in the effective area for $m = 10$.

For a rectangular test specimen, D is the diameter of a circle that expresses the characteristic size of the plate as follows:

$$D = \frac{l}{0.90961 + 0.12652\frac{h}{D_s} + 0.00168ln\frac{l - D_s}{h}} \quad (8)$$

where $l = 0.5\ (l_1 + l_2)$ and the other symbols are as defined Eq 1 and Eq 3.

10.2 *Plate Deflection*—The deflection for such a plate can be estimated from (**6**):

$$\delta = \frac{3F(1-\nu^2)D_L^2}{8\pi Eh^3}\left(\frac{D_S^2}{D_L^2}\left[1 + \frac{(1-\nu)(D_S^2 - D_L^2)}{2(1+\nu)D^2}\right] - \left(1 + ln\frac{D_S}{D_L}\right)\right) \quad (9)$$

10.3 *Mean, Standard Deviation and Percent Coefficient of Variation*—For each series of tests, the mean, standard deviation, and percent coefficient of variation for each measured value can be calculated as follows:

$$\text{Mean} = \bar{x} = \frac{\sum_{i=1}^{n} x_i}{n} \quad (10)$$

$$\text{Standard deviation} = \text{s.d.} = \sqrt{\frac{\sum_{i=1}^{n}(x_i - \bar{x})^2}{n-1}} \quad (11)$$

$$\text{Percent coefficient of variation} = \%\text{C.V.} = \frac{100(s.d.)}{\bar{x}} \quad (12)$$

where:

x_i = the valid measured value and n is the number of valid tests.

11. Report

11.1 Report the following:

11.1.1 The date and location of testing.

11.1.2 All relevant material data including vintage data or billet identification data. As a minimum, report the date the material was manufactured. For commercial materials, report the commercial designation.

11.1.3 Description of the stages of test specimen preparation including machining, heat treatments, coatings, or pre-test exposures applied either to the as-processed material or to the as-fabricated test specimens.

11.1.4 Type and configuration of the test machine (include drawing or sketch if necessary). If a commercial test machine was used, the manufacturer and model number are sufficient.

11.1.5 Material for and dimensions of the load and support rings.

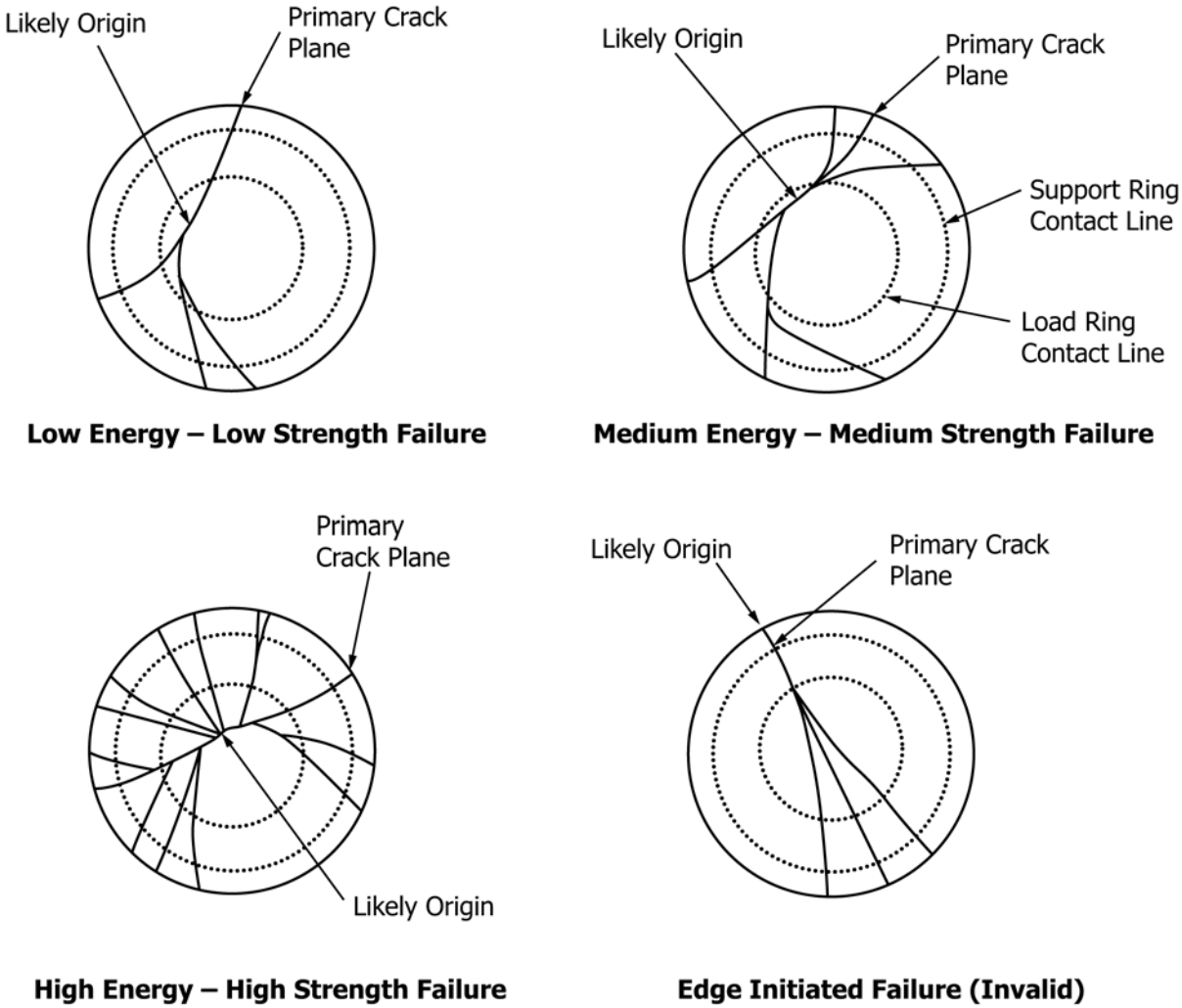

FIG. 4 Illustrations of Failure Patterns in Concentric Ring Test Specimens

11.1.6 Materials used as compliant and friction reducing layers, and the thickness of the layers, as applicable.

11.1.7 Type, configuration, and resolution of displacement measurement equipment used (include drawing or sketch if necessary). If a commercial extensometer was used, the manufacturer and model number are sufficient.

11.1.8 Test environment including relative humidity (Test Method E337), ambient temperature, and atmosphere (for example, ambient air, dry nitrogen, silicone oil, and so forth).

11.1.9 Test mode (load or displacement control) and applied test rate (load rate or displacement rate). The calculated stress rate should also be reported in units of MPa/s.

11.1.10 The values of Poisson's ratio and Young's modulus used in calculations.

11.1.11 Average diameter and thickness of each test specimen in units of mm.

11.1.12 Average surface roughness in units of μm, if measured, of the tensile face and direction of measurement relative to test specimen identification marks.

11.1.13 Preload applied to each test specimen in units of N.

11.1.14 Breaking load, F, of each test specimen in units of N.

11.1.15 Equibiaxial Strength, σ_f, of each test specimen in units of MPa.

11.1.16 Deflection at the Equibiaxial Strength, δ, of each test specimen in units of mm, if measured.

11.1.17 Location of fracture relative to the test specimen center, if applicable. Also, a summary of any fractographic analysis performed.

11.1.18 Number (n) of test specimens tested validly. In addition, report total number of test specimens tested (n_T) to provide an indication of the expected success rate of the particular test specimen geometry and test apparatus.

11.1.19 Mean, standard deviation, and coefficient of variation of the equibiaxial strength, σ_f, of the test lot in units of MPa.

12. Precision and Bias

12.1 Because of the nature of advanced ceramics and the lack of an extensive database, no definitive statement can be made at this time concerning precision and bias of this test method.

TABLE 1 Equibiaxial Test Results

Material	Equibiaxial Test Specimen Geometry (mm)				Equibiaxial Strength (MPa) σ_f	Number of Tests, n	Percent Coefficient of Variation, % C.V.
	D	D_s	D_L	h			
96 % Al_2O_3[A] (4)	23[B]	11	5	0.4	327[C]	42	11[D]
99.6 % Al_2O_3[E] (4)	23[B]	11	5	0.4	540[C]	48	7.6[D]
AlN[F] (4)	23[B]	11	5	0.4	323[C]	38	7.1[D]
SiC[G] (10)	30	23	12	2	206	36	14
Si_3N_4[H] (16)	45	40	10	2.2	501	6	5.8
AlN[I] (17)	36[J]	16	8	0.8	337	30	11[D]
SiC[G] (18)	30	23	12	2	325	36	12

[A] Grade ADS-96R, Coors Ceramic Company, Grand Junction, CO.
[B] Test specimens were square with an edge length of 19 mm.
[C] Weibull characteristic strength.
[D] C.V. estimated from the approximation for Weibull modulus m = 1.2/C.V. (19).
[E] Grade ADS-996, Coors Ceramic Company, Golden, CO.
[F] Carborundum Microelectronics, Phoenix, AZ.
[G] Hexoloy SA Alpha SiC, Carborundum, Niagara Fall, NY. Now Saint Gobain Industrial Ceramics, Latrobe, PA.
[H] Norton, NC 132, hot pressed silicon nitride, 1977 vintage.
[I] Toshiba Corp., Japan.
[J] Test specimens were square with an edge length of 30 mm.

12.2 Although no definitive statement can be made regarding the precision and bias, an indication of the precision (that is, percent coefficient of variation) is shown in Table 1 for a range of advanced ceramics.

12.3 Test results reported in Table 1 were generated by different investigators with different geometries and materials as chosen by the investigators.

13. Keywords

13.1 advanced ceramic; biaxial; concentric ring; equibiaxial; plate; strength

APPENDIXES

X1. ESTIMATION OF THE EFFECTIVE AREA AND EFFECTIVE VOLUME

X1.1 It is frequently of interest to calculate the "effective area" or "effective volume" of concentric ring test specimens. Assuming that the principal stresses control failure, the effective tensile surface area, *Ae*, and the effective tensile volume, *Ve*, can be calculated by numerical integration of the stress normalized to the maximum stress as a function of position according to the formulas:

$$A_e = \int_A \left(\frac{\sigma_1}{\sigma_{MAX}}\right)^m + \left(\frac{\sigma_2}{\sigma_{MAX}}\right)^m dA \qquad (X1.1)$$

and

$$V_e = \int_V \left(\frac{\sigma_1}{\sigma_{MAX}}\right)^m + \left(\frac{\sigma_2}{\sigma_{MAX}}\right)^m + \left(\frac{\sigma_3}{\sigma_{MAX}}\right)^m dV \qquad (X1.2)$$

where σ_1 and σ_2 are the tangential and radial stresses (1), and σ_{MAX} is the maximum stress as defined by Eq 7. The third principal stress, σ_3, is generally taken as zero for thin plates.

X1.2 For general purposes, the effective tensile surface area and effective tensile volume can be estimated to better than 3 % from (20):

$$A_e \cong \frac{\pi}{2} D_L^2 \left\{ 1 + \frac{44(1+\nu)}{3(1+m)} \frac{(5+m)}{(2+m)} \left(\frac{D_S - D_L}{D_S D}\right)^2 \left[\frac{2D^2(1+\nu) + (D_S - D_L)^2(1-\nu)}{(3+\nu)(1+3\nu)}\right]\right\} \qquad (X1.3)$$

and

$$V_e \cong Ae \left[\frac{h}{2(m+1)}\right] \qquad (X1.4)$$

for $m \geq 5$, $\nu \geq 0.17$, and $D_S/D_L = 0.5$, where *m* is the Weibull modulus. The other variables are as defined for Eq 1, Eq 2, and Eq 5. For $m \geq 5$ and $D_S/D_L = 0.2$, the estimates are better than 5 %. Ideally, the use of Eq X1.3 and X1.4 requires that the test data be grouped into surface failures and volume failures via fractography (Practice C1322), and the Weibull modulus be calculated with censored data analysis (Practice C1239).

X2. MULTILAYER CIRCULAR PLATES

X2.1 The strength of a circular plate made from layers with significantly different elastic constants can be determined from loading between concentric rings if the appropriate stress solution, elastic constants and assumptions are used. General formulations for thermal and mechanical loading of multilayer plates can be found in Refs 21-24 and specific formulas for normal stresses in Refs 24-27.

X2.1.1 Fig. X2.1 shows a diametrical section through the axis of symmetry of a thin, multilayer circular plate described by the cylindrical coordinates, r, θ, and z. The plate consists of n layers with individual thickness, t_i, where the subscript, i, denotes the layer number with layer 1 being at the bottom. The lower surface of layer 1 is located at $z = 0$, the interface between layers i and i+1 is located at h_i, and the upper surface of layer n is located at $z = h_n$ where h_n is the thickness of the plate. The relation between h_i and t_i is

$$h_i = \sum_{j=1}^{i} t_j \qquad (i = 1 \text{ to } n) \tag{X2.1}$$

X2.1.2 The circular plate is subjected to equibiaxial flexural loading with $z = 0$ and $z = h_n$ being the support and the load surfaces, respectively. The interfaces between layers are assumed to remain bonded during loading.

X2.1.3 For a multilayer plate, the equibiaxial stress within the inner load ring for a layer i is,

$$\sigma_i = \frac{-E_i(z - z_n^*)F}{4\pi(1-\nu_i)\Delta^*}\left[ln\left(\frac{D_S}{D_L}\right) + \frac{(1-\nu)(D_S^2 - D_L^2)}{2(1+\nu)D^2}\right] \tag{X2.2}$$

$$(\text{for } r = D_L/2 \text{ and } i = 1 \text{ to } n),$$

where D, D_S , D_L, F, E_i and ν_i are the specimen diameter, support ring diameter, load ring diameter, applied force, elastic modulus and Poisson's ratio of the i^{th} layer, respectively. The terms z_n^* and Δ^* are

$$z_n^* = \frac{\left[\sum_{i=1}^{n} \frac{E_i t_i}{1-\nu_i^2}\left(h_{i-1} + \frac{t_i}{2}\right)\right]}{\sum_{i=1}^{n} \frac{E_i t_i}{1-\nu_i^2}} \tag{X2.3}$$

$$\Delta^* = \sum_{i=1}^{n} \frac{E_i t_i}{1-\nu_i^2}\left[h_{i-1}{}^2 + h_i - 1^{t_i} + \frac{t_i^2}{3} - \left(h_{i-1} + \frac{t_i}{2}\right) z_n^*\right], \tag{X2.4}$$

and ν has the physical meaning of an average Poisson's ratio of the layers

$$\nu = \frac{1}{h_n}\sum_{i=1}^{n} \nu_i t_i \tag{X2.5}$$

When $i = 1$, h_{i-1} (i.e., h_0) in Eq X2.3 and Eq X2.4 is defined as zero. Depending upon the strength of the individual layers relative to the stress distribution through the thickness of the multilayer during testing, failure is expected to initiate from the layer in which the tensile strength is first exceeded. This assumes good bonding between layers. If relatively poor bonding exists, delaminating could occur. Fractography to understand the failure is recommended. In addition, the material needs to behave as a continuum and thus the solution may not be applicable to systems with large porosity or channels. In such case, the materials strength may better determine by testing individual layers rather than an assembly.

X2.2 Example Calculations and Comparison with Finite Element Analysis (FEA)

X2.2.1 For a bonded interface in multilayer systems, continuities of the displacement, the shear stress, and the stress normal to the interface are required. However, unless the material properties change continuously across the interface, the in-plane stress is not continuous at the interface. For monolayer plates, the maximum tension always occurs at the tensile surface (i.e., at $z = 0$). For multilayer plates, the equibiaxial stress is linear through the thickness in each individual layer; however, because of different elastic properties of the layers, the equibiaxial stress is discontinuous at the interface and the stress gradients are different. Fig. X2.2a-c show various stress distributions that can occur. In some cases, the maximum tension can occur at positions other than the tensile surface, as shown in Fig. X2.2c.

X2.2.2 For a D = 16 mm diameter bilayer plate consisting of a t_1 = 0.6 mm porcelain layer (E = 64 GPa, ν = 0.19) and a t_2 = 1.2 mm Alumina layer (E = 280 GPa, ν = 0.23) (total thickness

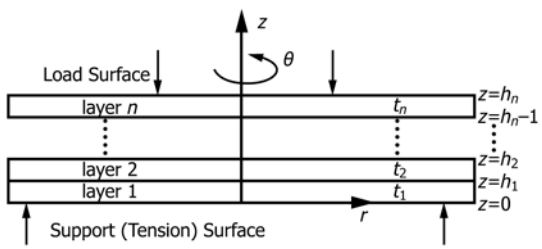

NOTE 1—Shows the coordinate system and the load and the support surfaces for an equibaxial flexural test.

FIG. X2.1 Diametrical Section of a Thin Multilayer Circular Plate

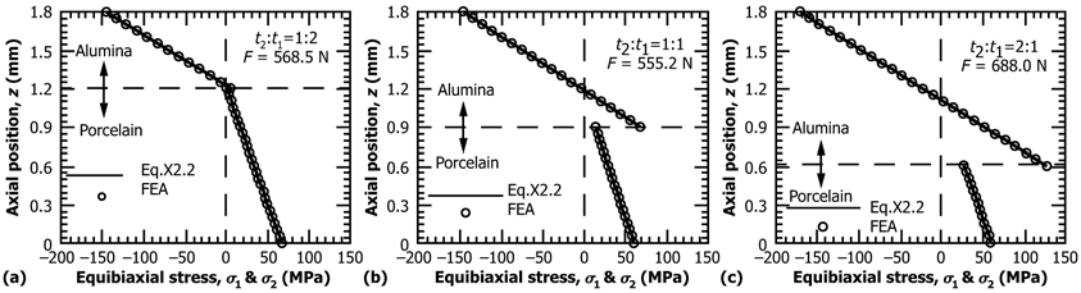

NOTE 1—These are subjected to ring-on-ring loading for alumina to porcelain layer thickness ratios of (a) 1:2 with F = 568.5 N, (b) 1:1 with F = 555.2 N, and (c) 2:1 with F = 688.0 N. Both analytical and finite element analysis (FEA) results are shown.

FIG. X2.2 The Equibiaxial Stress through the Thickness of 1.8-mm thick Porcelain/Alumina Bilayer Circular Plates

of $h_n = h_2 = 1.8$ mm) subjected to loading between $D_L = 5$ mm and $D_S = 11$ mm rings, the in-plane, principal stresses in the porcelain range from 59.9 MPa at the exterior surface to 27.5 MPa at the interface ($h_1 = 0.6$ mm) for an applied load 688 N as shown in Fig. X2.2c. For the alumina layer, the in-plane stresses range from 126.6 MPa at the interface (h_1) to – 171.8 MPa at the exterior surface ($h_2 = 1.8$ mm). Note that in this case, the maximum stress does not occur at the tensile surface, as is the case for monolayer plate, but at the interface between the layers. The location of the maximum tensile stress is determined by the elastic constants and layer thicknesses. If the isotropic solution (Eq 7) is used, a maximum stress of 113 MPa is predicted and the location is incorrectly assumed to be the plate tensile surface.

X2.3 Discussions

X2.3.1 It should be noted that an atomically sharp and smooth interface was assumed. This results in a discontinuity of the in-plane equibiaxial stress at the interface. In reality, roughness might exist at the interface and the layers may interact to form an interphase at the interface. In the presence of interfacial roughness, mechanical interlocking at the interface results in stress transfer between the neighboring layers at the interface and smoothing of the stress discontinuity at the interface. In the presence of an interfacial interphase, the material properties have a continuous variation at the interface which also smooths the stress discontinuity at the interface. It should also be noted that residual thermal stresses can exist in multilayer systems because of the thermomechanical mismatch between layers. Closed-form solutions for thermal stresses in elastic multilayers have been derived elsewhere (26 and 27), and resultant stresses in a multilayer can be obtained by superposing the thermal stresses on the stresses due to equibiaxial flexural loading.

REFERENCES

(1) Fessler, H., and Fricker, D. C., "A Theoretical Analysis of the Ring-on-Ring Loading Disk Test," *Journal of the American Ceramic Society*, Vol 67 [9], (1984) pp. 582-588.

(2) Wallace, J. S., Fuller, E. R., and Freiman, S. W., "Mechanical Properties of Aluminum Nitride Substrates," *NISTIR 5903*, National Institute of Standards and Technology, Gaithersburg MD, December 1996.

(3) Adler, W. F., and Mihora, D. J., "Biaxial Flexure Testing: Analysis and Experimental Results," *Fracture Mechanics of Ceramics*, Plenum Press, Vol 10, 1992, R.C. Bradt, Ed., pp. 227.

(4) Wereszczak, A. A., Kirkland, T.P., Breder, K., Lin, H.T., and Andrews, M.J., "Biaxial Strength, Strength-Size Scaling, and Fatigue Resistance of Alumina and Aluminum Nitride Substrates," *International Journal of Microcircuits and Electronic Packaging*, Vol 22, No. 4, 1999, pp. 446-458.

(5) Kao, R., Perrone, N., and Capps, W., "Large-deflection of the Coaxial-Ring-Circular-Glass-Plate Flexure Problem," *Journal of the American Ceramic Society*, Vol 54, No. 11, 1971, pp. 566-571.

(6) Vitmar, F. F., and Pukh, V. P., "A Method of Determining Sheet Glass Strength," *Zavodskava Laboratoriya*, Vol. 29, No. 7, 1963, pp. 863-867.

(7) Timoshenko, S. P., and Woinowsky-Krieger, S., *Theory of Plates and Shells, 2 ed.*, McGraw-Hill, New York, NY, 1959.

(8) Powers, L.M., Salem, J.A., and Weaver, A., "Stresses in Ceramic Plates Subjected to Loading Between Concentric Rings," *Fracture Resistance testing of Monolithic and Composite Brittle Materials*, *ASTM STP 1409*, J.A. Salem, G.D. Quinn, and M.G. Jenkins, Eds., ASTM International, 2002, pp. 30-45.

(9) Salem, J.A., "Mechanical Characterization of ZnSe Windows for use with the Flow Enclosure Accommodating Novel Investigations in Combustion of Solids (FEANICS) Module," *NASA TM 214100*, 2006.

(10) Salem, J. A., Nemeth, N. N., Powers, L. M., and Choi, S. R., "Reliability Analysis of Uniaxially Ground Brittle Materials," *Journal of Engineering for Gas Turbines and Power*, Vol 118, 1996, pp. 863-871.

(11) Quinn, G. D. and Braue, W.R., "Fracture Mechanism Maps for Advanced Structural Ceramics," *Journal of Materials Science*, Vol 25, 1990, pp. 4377-4392.

(12) Wiederhorn, S.M., Hockey, B.J. , Krause, Jr., R.F., "Creep and Fracture of a Vitreous-Bonded Aluminum Oxide," *Journal of Materials Science*, Vol 21, 1986, pp. 810-824.

(13) Salem, J. A., and Jenkins, M.G., "A Test Apparatus For Measuring the Biaxial Strength of Brittle Materials," *Experimental Techniques*, Vol. 23, No. 4, July/August 1999, pp. 19-23.

(14) Salem J., and Adams, M., "The Multiaxial Strength of Tungsten Carbide," *Ceramic Engineering and Science Proceedings*, Vol. 20, Issue 4, 1999, pp. 459-466.

(15) Manley, M., Erturk, T., Vaucamps, C. and Gailus, D. , "Four Point and Biaxial Flexure Strength of PZT Ceramics: A Probabilistic Approach," *Ceramic Engineering and Science Proceedings*, September-October B, 1994, pp. 885-894.

(16) Quinn, G. and Wirth, G., "Multiaxial Strength and Stress Rupture of Hot Pressed Silicon Nitride," *Journal of the European Ceramic Society*, Vol 6, 1990, pp. 169-177.
(17) Wallace, J. S., Fuller, E. R., Ueno, F., Kasori, M., Ohji, T., and Rafaniello, W., "Strength Measurement Metrology for A1N Substrates," To be published.
(18) Powers, L. M., Salem, J. A., and Choi, S.R., "Failure Prediction Using the Ring-on-Ring Test and the CARES/Life Integrated Design Program," *Reliability, Stress Analysis and Failure Prevention*, proceedings of the 1993 ASME Design Technical Conference, DE, Vol 55, 1993, pp. 55-63.
(19) Ritter, J. E., Bandyopadhyay, N., Jakus, K., "Statistical Reproducibility of Dynamic and Static Fatigue Experiments," *Ceramics Bulletin*, Vol 60, No. 8, 1981, pp. 798-806.
(20) Salem, J.A., and Powers, L.M., "Guidelines for the Testing of Plates," Proceedings of the 27th International Cocoa Beach Conference on Advanced Ceramics and Composites: B, *Ceramic Engineering and Science Proceedings*, Vol. 24, No. 4, Waltraud M. Kriven and H.T. Lin, Eds., January 2003, pp. 357–364.
(21) Grigolyuk, E.I., "Theory of Bimettalic Plates and Shells,"*Akademiia Nauk*, USSR, Inst. Mekhaniki, Inzhenernyi Sbornik, Vol. 17, 1953, pp. 69–120.
(22) Phister, K.S. and Dong, S.B., "Elastic Bending of Layered Plates," *Proc. Am. Soc. Civ. Eng*, Eng. Mech. Div., Vol. 85, No. 4, 1959.
(23) Ugural, A.C., *Stresses in Plates and Shells*, 2nd ed., McGraw-Hill, Boston, 1999
(24) Timoshenko, S. and Woinowsky-Krieger, S., *Theory of Plates and Shells*, McGraw-Hill, New York, 1959, pp. 51–54.
(25) Hsueh, C.H. and Luttrell, C.R., "Recent Advances in Modeling Stress Distributions in Multilayers Subjected to Biaxial Flexure Tests," *Compos. Sci. Technol.*,67, No. 2, 2007, pp. 278–285.
(26) Hsueh, C.H., Luttrell, C.R., and Becher, P.F., "Modeling of Multilayered Disks Subjected to Biaxial Flexure Tests," *Int. J. Solids Struct.,* 43, No. 20, 2006, pp. 6014–6025.
(27) Hsueh, C.H., "Thermal Stresses in Elastic Multilayer Systems,"*Thin Solid Films*, 418, No. 2, 2002, pp. 182–188.